To What Extent Multidecadal Changes in Morphology and Fluvial Discharge Impact Tide in a Convergent (Turbid) Tidal River

I. Jalón-Rojas, A. Sottolichio, V. Hanquiez, A. Fort, S. Schmidt

To What Extent Multidecadal Changes in Morphology and Fluvial Discharge Impact Tide in a Convergent (Turbid) Tidal River

I. Jalón-Rojas[1,2] (ID), A. Sottolichio[1], V. Hanquiez[1], A. Fort[3], and S. Schmidt[4] (ID)

[1]University of Bordeaux, EPOC, UMR5805, Pessac, France, [2]University of New South Wales, SARCCM, PEMS, Canberra, ACT, Australia, [3]Department of the Environment, Bordeaux Harbor, Bordeaux, France, [4]CNRS, EPOC, UMR5805, Pessac, France

Abstract Understanding nonstationary tides in tidal rivers is a major contemporary challenge. In particular, the response of river tides to natural developments in the estuary remains poorly investigated. This study analyzes the evolution of tidal characteristics over the last six decades in the Garonne Tidal River (GTR, SW France), in order to explore the effect of natural and human-induced morphological and hydrological changes on river tides. The tidal Garonne is an excellent example, as it has been subject to decreasing river discharges, natural morphological changes, and gravel extraction. Tidal range (TR), distortion (A_{M4}/A_{M2}), and asymmetry direction ($2\phi_{M2}-\phi_{M4}$) were calculated at four locations from the water level time series of 1953, 1971, 1982, 1994, 2005, and 2014. The annual time series of M_2 and M_4 amplitudes and phases were obtained through complex demodulation. Results reveal that both TR and $2\phi_{M2}-\phi_{M4}$ have increased since the 1950s. River flow modulates TR and A_{M4}/A_{M2} significantly. A long-term decrease in summer discharges from 200 ± 50 to 100 ± 50 m^3 s^{-1} would increase TR by $+11.5\%$ in the upper GTR. Natural morphological changes amplified TR and $2\phi_{M2}-\phi_{M4}$ by up to $+12$–15% between 1953 and 2014. TR and $2\phi_{M2}-\phi_{M4}$ doubled in the regions affected by gravel extraction between 1953 and 1971. Further, the persistence of mobile mud in the GTR increased TR seasonally but also interannually (by up to $+16\%$ in winter and spring of dry years). The potential impact of these changes on suspended sediments is discussed, revealing complex feedback between the evolution of hydrology, morphology, tides, and sediment trapping.

1. Introduction

Tides and freshwater discharge are the main physical forcings that generate flow in transitional waters, in particular in the upper estuarine zone hardly affected by salinity-induced density gradients or by waves (Barendregt & Swarth, 2013; Sassi & Hoitink, 2013). In estuarine channels subject to tidal currents, understanding the propagation of tidal waves and their interaction with river discharge is essential in assessing sediment transport and subsequent morphological changes. In the current context of climate change and anthropic impacts, tidal-river dynamics are becoming an increasingly important topic but are not yet well documented (Hoitink & Jay, 2016). Both interannual feedback from morphological changes and shifts in the hydrological regime can impact the hydrodynamic tidal regime; tidal wave propagation in estuaries is affected by the nonlinear effects induced by bottom friction, channel convergence in depth and width, and river discharge (Cai et al., 2014; Friedrichs & Aubrey, 1988; Godin, 1999; Savenije et al., 2008). Morphodynamics, hydrology, and estuarine hydrodynamics are therefore strongly coupled in long-term evolutionary processes (Lanzoni & Seminara, 2002; Moore et al., 2009).

Long-term changes in bottom friction, morphology, and river flow can indeed modify the amplification, damping, and asymmetry of tidal waves as they propagate landward. The tidal range in estuaries is the result of the balance between tidal wave amplification, which is induced by energy transfer from deep to shallow waters and from wide to narrow cross sections, and damping by bottom and river flow frictional dissipation (Friedrichs & Aubrey, 1994; Guo et al., 2015; Savenije et al., 2008). The nonlinear effects of these factors transform tides and tidal currents into an asymmetrical form, characterized by unequal rising and falling durations (vertical tidal asymmetry or tidal duration asymmetry) and unequal flood and ebb current peaks (horizontal tidal asymmetry or velocity skew; LeBlond, 1991; Speer & Aubrey, 1985). When the water level and velocity phases are 90° out of phase, a shorter flood duration relative to ebb results in faster flood

velocities, transfering the tidal prims in a shorter period; shorter ebb duration requires instead faster ebb currents (Friedrichs, 2010; Nidzieko, 2010). Estuaries are hence traditionally classified as flood dominant when rising tides are shorter in duration and the flood current stronger, or ebb dominant in the opposite case. Nidzieko and Ralston (2012) however highlighted that factors other than the duration asymmetry may influence the local velocity skew, such as phase lag between the surface gradient and local depth, river flow, and baroclinicity. Nonlinearities in wave propagation are manifest as the growth of subharmonics and overtides of the main astronomical constituents. In estuaries with predominantly semidiurnal tides, tidal distortion is reflected by the interaction of the principal lunar M_2 component of the water level (for the vertical asymmetry) and the current velocity (for the horizontal asymmetry) with its overtides, i.e., M_4 and M_6 (Friedrichs & Aubrey, 1988; Guo et al., 2016; Lanzoni & Seminara, 1998; Speer & Aubrey, 1985).

Although many studies have evaluated tidal distortion in different estuaries (e.g., Dronkers, 1992; Fortunato & Oliveira, 2005; Neill et al., 2014; Prandle, 1985; Toublanc et al., 2015; Yoon & Woo, 2013), river-modulated tides upstream of the limit of salinity intrusion have gained attention only recently. The development and widespread use of nonstationary tidal analysis methods (Appendix A gives a brief overview of methods used to calculate tidal components) match the present-day research effort to understand the interactions of river discharge with tides. River discharge influences both the tidal and subtidal water levels (Alebregtse & de Swart, 2016; Henrie & Valle-Levinson, 2014; Jay & Flinchem, 1997; Ross & Sottolichio, 2016), enhances tidal friction, thereby damping tidal energy and tidal range (Cai et al., 2012, 2014; Godin, 1991; Savenije et al., 2008), decreases wave celerity (Godin, 1985; Savenije et al., 2008), and controls tidal interactions by dissipating the principal tidal constituents and favoring energy transfer from the principal bands to the lower and higher frequencies (Guo et al., 2015, 2016). This generation of overtides and compound tides is favored until they reach a point upstream where they are damped more rapidly by friction than they are generated through the nonlinear interactions (Matte et al., 2014). Moreover, Losada et al. (2017) highlighted the fact that river flow can also influence the propagation of tides by modulating the suspended sediment stratification of the water column: a higher stratification restricts frictional influence to the bottom layers and partially decouples the overlying flow from the bottom, increasing in turn tidal wave celerity.

Notwithstanding these recent advances, there is still progress to be made in understanding river tides. A key challenge is to explain and predict the evolution of tidal-river dynamics in response to contemporary hazards (Hoitink & Jay, 2016) such as climate change. Most studies evaluating long-term changes in tidal properties in estuaries have examined the impact of morphological changes resulting from human intervention in the system: deepening (de Jonge et al., 2014; van Maren et al., 2015; Winterwerp & Wang, 2013), narrowing (Moore et al., 2009; Winterwerp et al., 2013), and weirs (Chernetsky et al., 2010; Schuttelaars et al., 2013). All have demonstrated that both the loss of intertidal areas by deepening and narrowing, and the shortening of the estuary length increase tidal range and favor a deeper penetration of tides up-estuary, which in turn increases turbidity in the upper reaches significantly. However, less attention has been paid to estuaries in which direct human intervention has been less drastic and the morphology has evolved under the significant control of natural boundary conditions (Moore et al., 2009). To our knowledge, no study has dealt with the impact of interannual hydrological changes or the simultaneous effects of hydrological and morphological changes.

The general objective of this work is to explore the effect of natural and human-induced morphological and hydrological changes on the propagation of tides in the Garonne Tidal River (GTR, SW France, Figure 1). The Gironde Estuary and its tributaries, the tidal Garonne and Dordogne Rivers, are indeed a clear example of a large fluvial-estuarine system subject to multiple pressures. During the last decades, its incoming river discharge has decreased during both the wet and dry seasons (Caballero et al., 2007; Chevalier et al., 2014; Jalón-Rojas et al., 2015). The estuary (downstream from the confluence) has maintained its general shape and undergone relatively moderate natural morphological change compared with other European macrotidal systems (Sottolichio et al., 2013). However, some sections of the upper GTR were deepened between the 1960s and 1980s by gravel extraction (Figure 1; Castaing et al., 2006). River flow is an important factor forcing the variability in the subtidal water level (Ross & Sottolichio, 2016) and in the turbidity (Jalón-Rojas et al., 2017), especially in the GTR. Jalón-Rojas et al. (2015) further demonstrated that the long-term hydrological changes are one of the factors contributing to the intensification of the turbidity maximum in the upper estuary in the last 50 years. To date, the impact of the different pressures on the evolution of tides has not been analyzed.
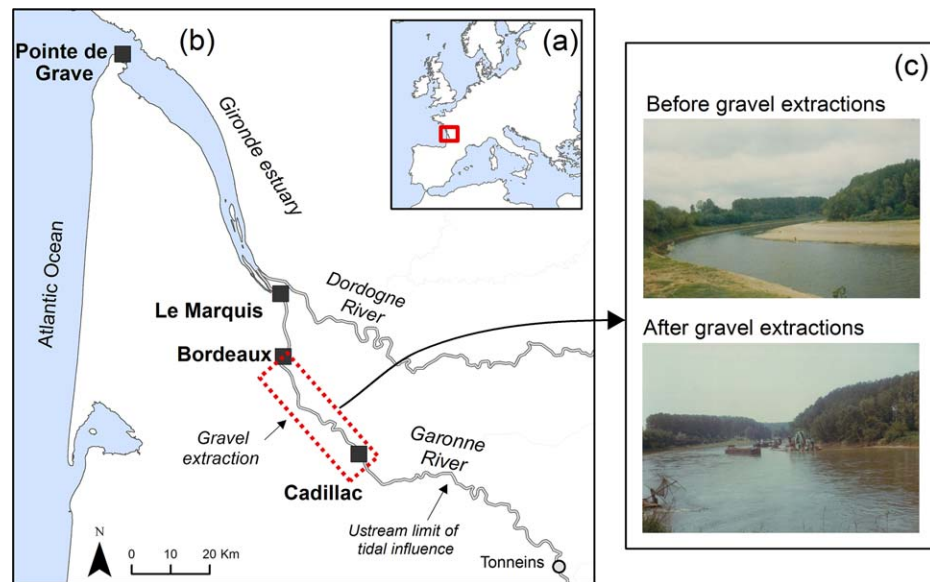
Figure 1. (a) Location of the study site in the southwest of France and (b) the Gironde Estuary and its two tidal rivers, the Garonne and Dordogne. Black squares show the tidal gauges (with distance from the mouth): Pointe de Grave (0 km, mouth of the estuary), Le Marquis (82 km), Bordeaux (100 km), and Cadillac (138.5 km). The gray circle shows the Tonneins hydrometric station. The dashed red rectangle shows the zone affected by gravel extraction between the 1960s and the 1980s. (c) Example of the Garonne's banks before and after gravel extraction works (*source*: http://atlas-paysages. gironde.fr).

The specific aim of this paper is to evaluate and understand the evolution of the tide characteristics, i.e., the tidal range and asymmetry, over the last six decades in the GTR. This study is based on the analysis of annual time series of continuous water level recorded by four tidal gauges during six different years between the 1950s and the present. First, we describe the multidecadal evolution of the tidal patterns. The effects of river flow and morphological changes on the tidal range and asymmetry, and their implications are then discussed. This provides further insight into prospective changes in the tides and a basis for evaluating the impact of morphological and hydrological changes on suspended sediment transport patterns.

2. Study Site and Field Data

2.1. The Garonne Tidal River

The Garonne Tidal River (GTR) is located in southwest France (Figure 1a). It meets the Dordogne tidal river forming the Gironde estuary (Figure 1b), which has a regular funnel shape of length 75 km between the Atlantic coast and the rivers' confluence. From this confluence, the GTR extends 95 km inland to the upstream limit of tidal influence. The width of the Gironde-Garonne system varies from 11.3 km near the mouth (Huybrechts & Villaret, 2012) to 125 m or less near the limit of tidal influence. Nowadays, the Garonne brings to the Gironde a daily discharge ranging from 50 to 4720 $m^3 s^{-1}$ (data for the period from 2005 to 2014, hydro.eaufrance.fr). Tides at the mouth are semidiurnal, with a tidal range varying from about 2.5 to 5 m on mean neap/spring tides (Bonneton et al., 2015). As the tidal wave propagates up the estuary, both the tidal amplitude and the asymmetric shape of the wave are amplified. Rising waters become shorter and flood currents stronger, i.e., the estuary is flood dominant (Allen et al., 1980). For low river discharges, the convergence effects exceed the frictional effects from the mouth up to around Cadillac (Figure 1b), where tides reach their maximum amplitude (up to 6.3 m on spring tides) and current velocities (Bonneton et al., 2015). Further upstream, the tidal range and current velocities decay in the fluvial narrow sections. The limit of maximum tidal amplitude is expected to move depending on river discharge and the phase of the neap-spring tidal cycle; the increasing dissipation on spring tides damps the tide earlier than on neap tides (Matte et al., 2017). In terms of tidal harmonics, the principal M_2 component increases linearly by 0.59 cm/km from the estuary mouth to Bordeaux (Ross & Sottolichio, 2016).

Both the hydrology and morphology of the Gironde Estuary have evolved over time. Over the last six decades, the Garonne mean annual discharge has decreased by 31%, from 650 to 445 m^3 s^{-1} (Jalón-Rojas et al., 2015), the number of extreme river floods has decreased and the duration of dry periods increased (Schmidt et al., 2017). This hydrological regime shift is attributed to both climate change and the increase in surface irrigation (Boé et al., 2009; Mazzega et al., 2014). As in the other main French watersheds, the Garonne flow is correlated with the North Atlantic Oscillation (NAO; Chevalier et al., 2014). The Gironde's morphological evolution is however poorly documented. A previous study of the bathymetry of the Gironde (from the mouth to the river confluence) covering the period 1962–1994 revealed that the Gironde had maintained its section and shape, and undergone only moderate morphological changes. The only remarkable pattern was the continuous landward migration of the main area of sedimentation: in the period 1962–1970 the sedimentation area was located in the lower estuary, but in the period 1970–1994 it shifted to the upper estuary (Sottolichio et al., 2013). This is consistent with the upstream shift of the location of turbidity maximum zone that, for constant morphology and tidal features, is related to the decrease in the discharge (Jalón-Rojas et al., 2015). In addition, the GTR between Bordeaux and Cadillac was subject to significant gravel extraction between 1956 and 1980 (Castaing et al., 2006). This deepened the channel and changed the river banks from wide gravel beaches to steep edges (Figure 1c). Accurate bathymetries are not available for this period, but occasional observations reported that the concerned sections underwent an average deepening of 1–2 m. However, some sections were deepened by up to 4 m, and even up to 6 m close to Cadillac; the sections were refilled by fine sediments, thus reducing the bottom roughness (Castaing et al., 2006).

2.2. Data

This work is based on two sets of data:

a. Water level measurements at four stations (Figure 1): Pointe de Grave at the Gironde's mouth, and Le Marquis, Bordeaux, and Cadillac in the GTR. The Bordeaux Harbor Authority provided these data as paper records for the years before 1980, and in digital form after. At Cadillac, measurements were stopped in 1995, and all the data are in paper form. The choice of annual time series was a compromise between the effort required to digitize paper-based tidal signals and having a good representation of the different hydrological conditions (floods, dry periods, and wet/dry years). Based on data quality, we have selected water level time series from 6 years distributed over the last six decades: 1953 (1956 for Cadillac), 1971, 1982, 1994, 2005, and 2014.
b. Daily river discharge recorded at Tonneins (Figure 1) for the same years. The Tonneins station is situated upstream of the limit of tidal propagation. Records were supplied by the DREAL Midi-Pyrénées and are available on the national French website www.hydro.eaufrance.fr/.

3. Methods

3.1. Time Series Digitization

We digitized the water level time series using ArcGIS for Desktop v10.3 software (ESRI, 2014). First, paper sheets were scanned and their digital versions georeferenced in the cylindric conform Mercator projection system. This allowed us to identify the temporal scale and the subsequent concatenation of tidal signals. Secondly, the tidal signals were manually digitized. Finally, a sequence of pairs of time and water level were obtained from the geoprocessing steps.

3.2. Postprocessing

In order to characterize the tides, two parameters were calculated from water level time series: tidal range and vertical asymmetry. The tidal range (TR) was estimated in three steps. For each annual time series: (a) water level was high-pass filtered to remove the variations at subtidal levels; (b) individual tidal waves were identified from zero upcrossing points; then (c) tidal range is calculated as the difference between the high and low waters. The amplification of the tide in the estuary (TR/TR$_{mouth}$) was calculated as the ratio of the tidal range at a given station and TR$_m$, the tidal range at Pointe de Grave (at the estuary mouth, the reference). The use of this parameter ensures that the causes of the interannual tidal range evolution are intrinsic to the estuary rather than of oceanic origin.

The vertical tidal asymmetry was assessed from the interactions of the M_2 and M_4 tidal components. Following Friedrichs and Aubrey (1988), the ratio of the amplitudes of these components (A_{M4}/A_{M2}) is an estimate of the degree of tidal distortion, and their relative phase ($2\phi_{M2}$-ϕ_{M4}) determines the direction of the asymmetry: flood dominant if the relative phase is in the range 0°–180° (90° indicates maximum flood dominance); and ebb dominant if the relative phase is in the range 180°–360° (270° for maximum ebb dominance).

In order to evaluate the nonstationary interactions between tide and river discharge, the amplitudes A and phases ϕ of the semidiurnal and quatediurnal frequency bands (D_2 and D_4) were calculated over time using the Method of Complex Demodulation (Boon, 1992; Gasquet & Wootton, 1997), a nonstationary method based on a wavelet approach. This method resolves tidal species (e.g., D_2 and D_4 tidal bands) but not the specific tidal harmonics within species (e.g., M_2, S_2, M_4, and MS_4). We discarded the use of other nonstationary methods; the short-time harmonic analysis (Godin, 1999) provides inaccurate results when river discharge variability is high (Godin, 1999; Jay & Flinchem, 1997), and the nonstationary harmonic analysis (Matte et al., 2013) requires several years of records (Hoitink & Jay, 2016; Matte et al., 2013), which are not available for the Gironde. The advantages and limitations of several tidal analysis methods are summarized in the Appendix A.

Complex Demodulation assumes that the time series X(t) are composed of a nearly periodic signal with frequency σ and a nonperiodic signal Z(t):

$$X(t) = A(t)\cos(\sigma t + \phi(t)) + Z(t)$$

The nearly periodic signal represents the tidal component of frequency σ ($2\pi/12.48$ rad h^{-1} for D_2 or $2\pi/6.24$ rad h^{-1} for D_4) whose amplitude A and phase ϕ we want to calculate. The amplitude and phase are allowed to vary with time but slowly compared to the frequency σ. These parameters are estimated in three steps:

a. The original time series is multiplied by $e^{-i\sigma t}$ in order to shift the frequency of interest to zero:

$$Y(t) = X(t)e^{-i\sigma t} = \frac{A(t)}{2}e^{-i\phi(t)} + \frac{A(t)}{2}e^{-i(2\sigma t + \phi(t))} + Z(t)e^{-i\sigma t}$$

b. Y(t) is then low-pass filtered to remove frequencies at or above σ, i.e., the terms $\frac{A(t)}{2}e^{-i(2\sigma t + \phi(t))} + Z(t)e^{-i\sigma t}$ are removed to give

$$Y'(t) = \frac{A'(t)}{2}e^{-i\phi'(t)}$$

c. The corresponding A'(t) and ϕ'(t) are calculated from the Inverse Fourier Transform of the filtered spectrum Y'(t):

$$A'(t) = 2|Y'| = 2\left(\text{Re}(Y')^2 + \text{Im}(Y')^2\right)^{1/2}$$

$$\phi'(t) = \text{atan}\left(\frac{\text{Re}(Y')}{\text{Im}(Y')}\right)$$

The estimated amplitude and phase will be used from now without the prime. For further information about the method, the reader is referred to Bloomfield (2004).

4. Results

4.1. Hydrology of the Investigated Years

The six selected years have contrasting hydrological features (Figure 2). The years 1953 and 2005 were very dry, with annual mean-daily river flows lower than 350 m^3 s^{-1}. In 2005, the daily river flow only exceeded 800 m^3 s^{-1} on 6 days, and never reached 1,000 m^3 s^{-1} (Figure 2e). In contrast, the year 1953 had several
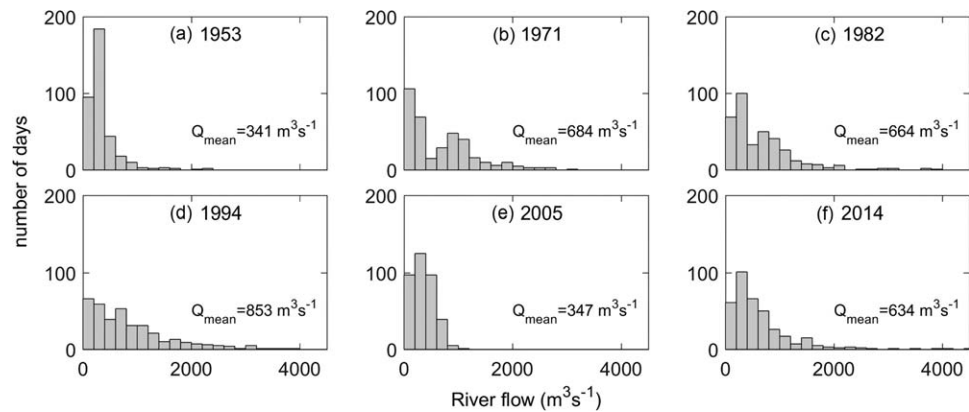
Figure 2. Histograms (number of days per year) of the Garonne's daily river flow (intervals of 200 m^3 s^{-1}) for the years 1953, 1971, 1982, 1994, 2005, and 2014. Q_{mean} is the mean annual river flow.

winter floods, with a maximum river flow of 2,500 m^3 s^{-1}. Even so, this was actually the driest year from the 1950s to the 1980s. The years 1971 and 1982 were more representative of the years before the 1990s from a hydrological point of view, and are comparable with current wet years such as 2014 (Figures 2b–2f). These 3 years were characterized by mean-daily river flows in the range 630–680 m^3 s^{-1}, by wet winters with large floods, but also by long periods of river flow below 400 m^3 s^{-1}. The year 1994 was the wettest, with a mean-daily river flow of 853 m^3 s^{-1} and a short dry period (Figure 2d).

4.2. Multidecadal Evolution of Tidal Range

The evolution of tidal range from 1953 to the present has followed different patterns at the Gironde's mouth and in the GTR. At Pointe de Grave, the tidal ranges were fairly similar for 1953 and 2014 (the first and last years of observation), reaching minimum and maximum values of 1.5 and 5.2 m, respectively (Figure 3b). In contrast, TR was strongly amplified over the same period in the GTR (Figures 3c and 3d), reaching maximum values of 5.6 m in 1953 and 6.5 m in 2014 at Bordeaux (5.4 m in 1953 and 6 m in 2014 at Le Marquis). In addition, while the tidal range showed no seasonal variability at Pointe de Grave, there was a
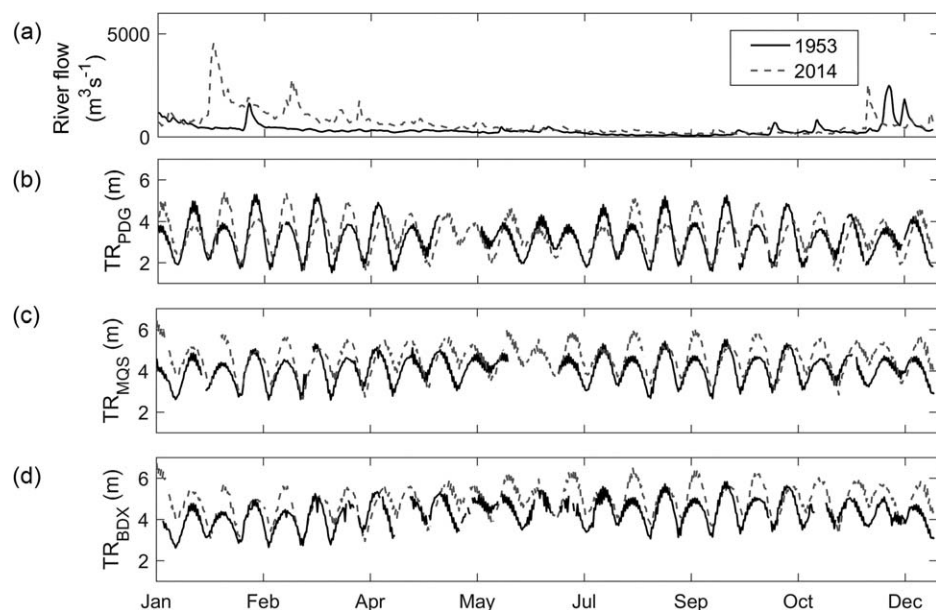

Figure 3. Annual time series of (a) river flow, and of the tidal range at (b) Pointe de Grave, (c) Le Marquis, and (d) Bordeaux for the years 1953 and 2014.
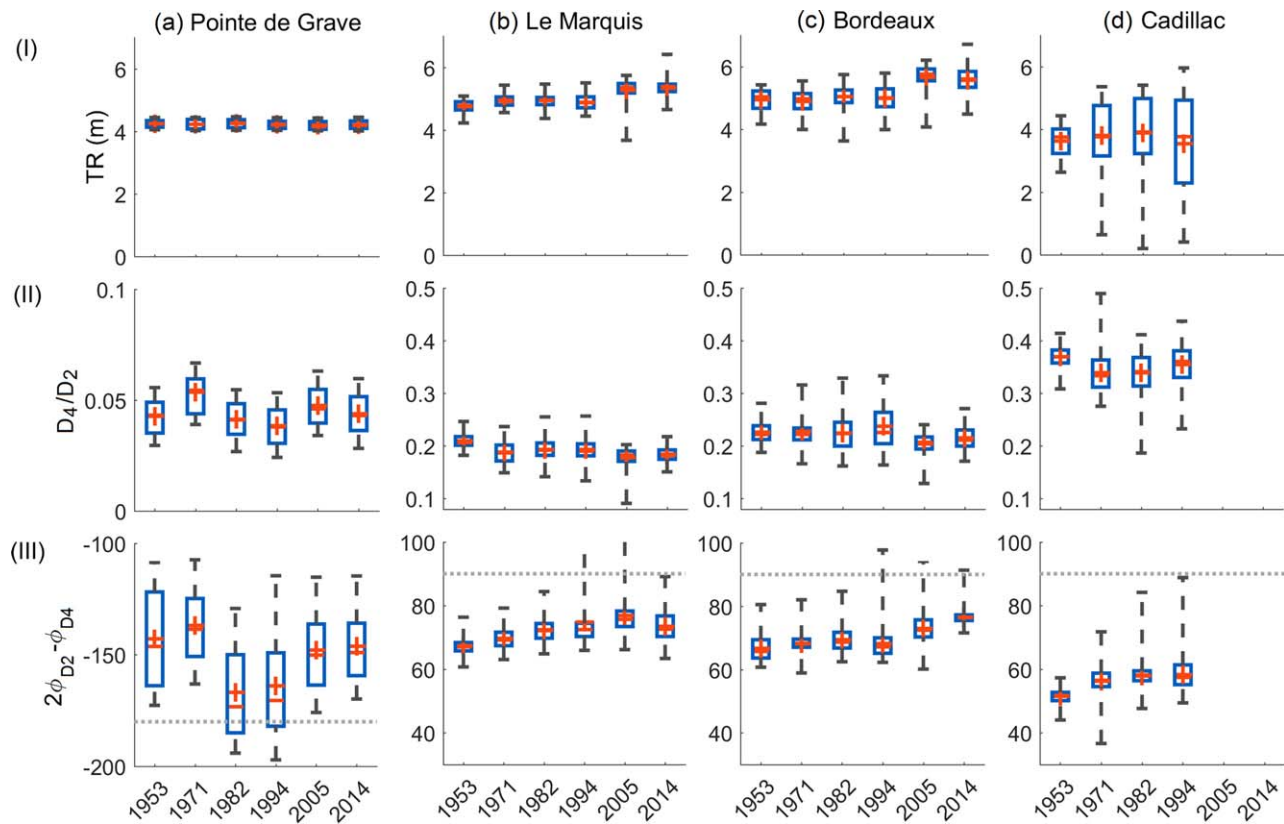
Figure 4. Mean (red cross), median (red bars), percentiles 25–75 (blue bars), and minimum/maximum (black bars) values of (I) tidal range, (II) tidal distortion A_{D4}/A_{D2}, and (III) tidal asymmetry direction $2\phi_{D2}-\phi_{D4}$ at (a) Pointe de Grave, (b) Le Marquis, (c) Bordeaux, and (d) Cadillac for a tidal range at the mouth comprised between 4 and 4.5 m. Light gray dotted lines at (III) indicate the lowest limit of ebb dominance in (a) and the highest limit of flood dominance in (b)–(d). For tidal distortion (II) and asymmetry direction (III), the scale of the vertical axis for Pointe de Grave (a) is different from that of the other three stations (b–d).

strong increase during low river discharge periods at Le Marquis and Bordeaux (Figures 3b–3d). For example, during the wet year of 2014, the maximum tidal ranges at Bordeaux in winter and summer were 5.6 and 6.5 m, respectively. The absence of TR changes at the mouth (Le Verdon) indicates that the causes of this tidal wave amplification must be sought within the estuary. Given that higher river flows decrease the tidal range in the upper sections (Guo et al., 2015), the higher tidal ranges in the GTR during the wet winter of 2014 than during the dry winter of 1953 may imply that other factors, such as morphology or bottom roughness, have also affected the tidal range over years.

In order to quantify the evolution of tidal increases in the GTR over the last decades, Figure 4I summarizes the main characteristics (mean and percentiles) of the tidal range during each investigated year at the four stations; the corresponding tidal ranges at the mouth were between 4 and 4.5 m. A tidal range of 4–4.5 m at Pointe de Grave increased at Le Marquis up to 4.2–5.1 m in 1953 and up to 4.6–6.4 m in 2014 (4.2–5.4 m in 1953 and 4.5–6.7m in 2014 at Bordeaux; Figure 4Ia–4Ic). At Le Marquis and Bordeaux, the trends were similar: the mean tidal range increased by +14% between 1953 and 2014. However, this increase took place over two distinct periods: around 2–3%, from 1953 to 1994; and around 12% between 1994 and 2005.

At Cadillac (Figure 4Id), the uppermost station, the tidal range increased or decreased depending on river flow. Tidal ranges of 4–4.5 m at the mouth reached a minimum of 2.6 m and a maximum of 4.4 m in the dry year of 1953 (0.4 and 6 m, respectively, for the wet 1994). This strong dependence of tidal range on river flow in the upper GTR, together with the contrasting hydrological regimes of the different years (section 4.1), led to a different pattern in the multidecadal tidal range evolution at Cadillac. However, the maximum values of the tidal range, which were associated with the lowest river flows, increased by +36% between 1953 and 1994 (Figure 4Id); the multidecadal tidal wave amplification at Cadillac was significantly higher than in the lower reaches of the GTR during dry seasons.

The evolution of the tidal range in the GTR was therefore mainly characterized by a net increase but with different patterns in the lower and upper reaches. These results suggest that not only hydrological but also geomorphological changes could have caused this evolution. The impact of each pressure on TR is discussed in section 5.

4.3. Multidecadal Evolution of Tidal Asymmetry

The vertical tidal asymmetry also varied between the mouth and the tidal river. Figures 4II and 4III compare the main characteristics (mean, percentiles) of tidal distortion (A_{D4}/A_{D2}) and asymmetry direction ($2\phi_{D2}$-ϕ_{D4}) over the studied years at the different stations, again corresponding to a tidal range of between 4 and 4.5 m at the mouth. The tides were virtually undistorted ($A_{D4}/A_{D2} \ll 0.1$) and ebb dominant ($-200° < 2\phi_{D2}$-$\phi_{D4} < -100°$) at Pointe de Grave (Figures 4IIa and 4IIIa). In contrast, the tides in the GTR were distorted, with A_{D4}/A_{D2} up to 0.5, and flood dominant, $60° < 2\phi_{D2}$-$\phi_{D4} < 130°$ (Figures 4IIb–4IId and 4IIIb–4IIId). A_{D4}/A_{D2} was roughly constant over the years at Pointe de Grave, but increased up estuary (Figure 4IIa–4IId). $2\phi_{D2}$-ϕ_{D4} showed no significant trend with time at Pointe de Grave. At this station, $2\phi_{D2}$-ϕ_{D4} was closer to the maximal ebb dominant condition during 1982 and 1994 (Figure 4IIIa). In contrast, $2\phi_{D2}$-ϕ_{D4} rose progressively over decades in the GTR, becoming increasingly closer to the maximum flood dominant conditions (Figures 4IIIb–4IIId). Mean values increased by 11% and 17% at Le Marquis and Bordeaux, respectively, between 1953 and 2014. At Cadillac, an increase of 14% occurred between 1953 and 1994, showing a higher intensification of flood dominant conditions there between the 1950s and the 1990s. Even then, the flood dominance at Cadillac was the weakest compared to the lower stations, probably due to the enhanced effect of river flow. Just like tidal range, the vertical tidal asymmetry in the tidal Garonne seems to evolve temporally and spatially under the influence of hydrology and morphology.

5. Discussion

5.1. Impact of Long-Term Hydrology Changes on Tide Evolution
5.1.1. Fluvial-Tidal Interactions

The influence of river flow on tidal range and vertical asymmetry in the GTR has been explored here in order to determine the impact of long-term hydrological changes on tidal propagation. The effects of river flow on tidal dynamics are known, mostly based on analytical solutions, but are still poorly quantified with real observations: river flow attenuates tidal energy; enhances tidal friction, thus damping tidal amplitudes; alters tidal phases; and modulates tidal interactions, generating overtides and compound tides (Godin, 1985; Guo et al., 2015; Jay & Flinchem, 1997; Sassi & Hoitink, 2013). Kukulka and Jay (2003) developed a regression model for tidal hindcasting by considering a very broad range of river discharges. Recent analytical solutions have considered the effect of river discharge on tidal dynamics primarily through the friction term, without simplifying the equations; these were able to accurately reproduce tidal damping in the upper estuary, where the ratio of the river-flow to tidal-flow amplitude is substantial (Cai et al., 2012, 2014). Unlike these analytical works, we first quantify and illustrate the impact of river flow on tidal decay and deformation based on the time series.

For this purpose, the tidal range, distortion and vertical asymmetry direction at the four stations are represented as functions of the river flow and the tidal range at the mouth TR_{mouth} (Figure 5). Only a 1 year data series was used to eliminate the potential effects of interannual morphological changes. The year 1994 was selected because it was characterized by a large range of river discharges (Figure 2d) and is the most recent year counting with water level data at Cadillac. Unlike the estuary mouth, where river flow has no influence on TR, the effect of tidal damping with increasing river discharges is evident at the three stations in the GTR (Figure 5I), in particular at Cadillac, consistent with other modeling studies in tidal rivers (Gallo & Vinzon, 2005; Godin, 1991; Horrevoets et al., 2004). For river discharges lower than 150 m^3 s^{-1}, a TR_{mouth} of 4.5 m increased to 5.4 (20%), 5.9 m (32%), and 6 m (33%) at Le Marquis, Bordeaux and Cadillac, respectively. However, for river discharges higher than 3,500 m^3 s^{-1}, a TR_{mouth} of 4.5 m now gave the same value, 4.5 m, at Le Marquis and Bordeaux, but decreased to below 0.8 m (a decrease of 82%) at Cadillac. TR could therefore be 7.5 times higher during dry periods than during wet periods in the region of Cadillac (138.5 km from the mouth over a total estuarine length of 180 km) for a same TR_{mouth} (Figure 5Id). It is difficult to compare the TR variability under the varying river discharges of different systems, because this depends on the longitudinal position. However, there appears to be a huge variation in the GTR compared to analogous upper
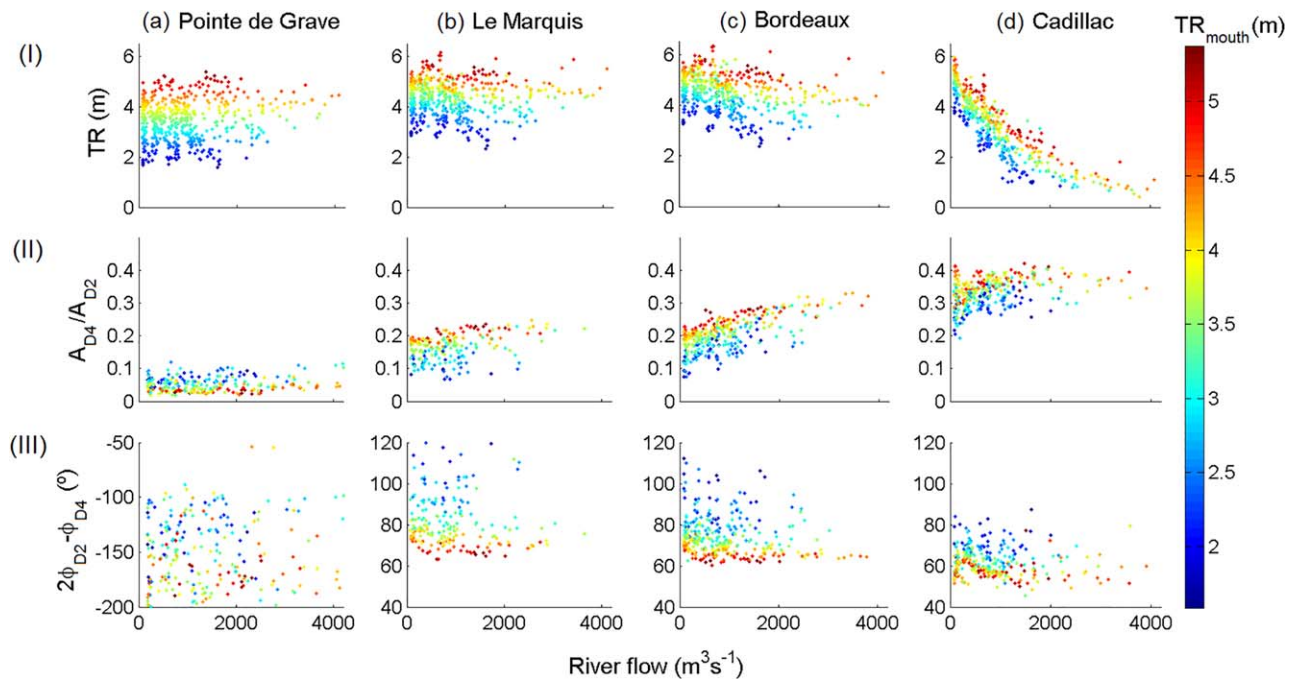
Figure 5. (I) Tidal range (TR), (II) tidal distortion (A_{D4}/A_{D2}), and (III) tidal asymmetry direction ($2\phi_{D2}-\phi_{D4}$) for the year 1994 as a function of river flow and tidal range at the mouth (colorbar) at (a) Pointe de Grave, (b) Le Marquis, (c) Bordeaux, and (d) Cadillac.

sections of other documented tidal rivers. For example, in the Guadalquivir Estuary (Wang et al., 2014), the tidal range during dry periods is twice that during river floods at Seville (77 km over 110 km). In the Yangtze Estuary (Guo et al., 2014), the tidal range is at most 1.7 times higher during dry periods in upper reaches. This also implies that the river flow strongly influences the section from which tides begin to be sharpy damped: around Bordeaux (100 km over 180 km) during river floods and upstream Cadillac (138.5 km over 180 km) during dry periods. This result contrasts with the damping trends of tidal components in the St. Lawrence estuary that follow a sharp decrease from a same section, characterized by a rapid increase in bottom slope (163.5 km over 300 km), whatever river flow (Matte et al., 2014). The results of the St. Lawrence estuary support the idea previously reported by Sassi et al. (2012) that sharp changes in morphology set the boundary between river-dominated and tide-dominated parts. This is also the case in the Yangtze Estuary (Guo et al., 2014) where tidal range decreases abruptly from the section where the narrowing increases significantly. In the GTR, where there are no drastic morphological ruptures but where the bottom slope begins to increase upstream from Cadillac, the position of this boundary depends very sensitively on the river flow.

Tidal distortion, almost uninfluenced by river flow at the estuary mouth, increases up-estuary in relation with the energy transfer from D_2 to D_4, as both the bottom and river flow enhance friction in the upper reaches (Figure 5II). In the GTR, higher river flows favor the growth of overtides and lead to longer ebb phases, and therefore to higher A_{D4}/A_{D2}. For low tidal ranges, this parameter doubles during high river discharges at Le Marquis and Bordeaux compared to dry periods (Figures 5IIb and 5IIc). At Cadillac, A_{D4}/A_{D2} increases with river flow up to 1,800 $m^3 \ s^{-1}$, then decreases slightly (Figure 5IId). This agrees with the idea of Matte et al. (2014) that M_4 can be damped more rapidly by discharge than it is created from nonlinearities in the uppermost estuarine region. Even if there are no data to verify the decrease in A_{D4}/A_{D2} upstream Cadillac, the damping of A_{D4}/A_{D2} during river floods at this station gives a first insight of this effect. Guo et al. (2015) showed a similar variation of A_{D4}/A_{D2} with river flow in the Yangtze Estuary. In the lower Yangtze (160 km over 650 km), A_{D4}/A_{D2} increases from low to high discharges, as do those at Le Marquis and Bordeaux (82 km and 100 km over 180 km). In the upper Yangtze (430 km over 650 km), A_{D4}/A_{D2} increases compared to the lower reaches during dry seasons but decreases with river flow due to the river-enhanced subtidal friction, which attenuates tidal energy and the growth of overtides as mentioned previously. In the GTR, this effect becomes noticeable at Cadillac (138.5 over 180 km). This spatial lag in the effect of river flow
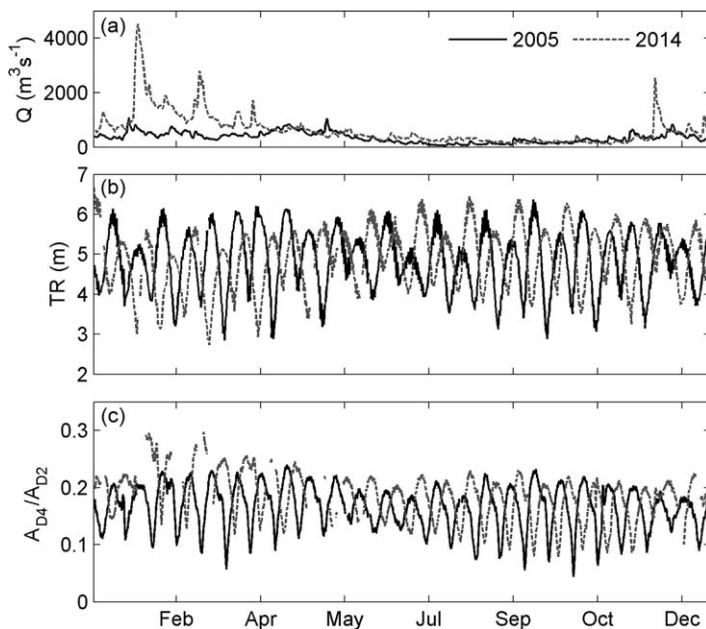
Figure 6. Time series of (a) river flow, (b) tidal range, and (c) tidal distortion at Bordeaux during 2005 (solid black line) and 2014 (gray dashed line).

on A_{D4}/A_{D2} between the GTR and the Yangtze or the St. Lawrence Estuaries can be explained by the fact that the Gironde is hypersynchronous (Castaing & Allen, 1981), meaning that its tidal ranges and currents are amplified toward the head of the estuary; its river flow is up to 10 and 20 times lower than that in the St. Lawrence Estuary and the Yangtze Estuary, respectively.

River flow does not influence the tidal asymmetry direction (Figure 5III), as previously observed by Gallo and Vinzon (2005) in the Amazon River. In fact, the phase difference $2\phi_{D2}-\phi_{D4}$ only shows the transition from an ebb dominant asymmetry at the mouth to a flood dominant asymmetry ($0 < 2\phi_{M2}-\phi_{M4} < 180$; Friedrichs & Aubrey, 1988) in the estuary. Only at Cadillac, increasing river flows slightly reduce $2\phi_{D2}-\phi_{D4}$ and therefore the flood dominance, consistent with the effect of river flow in attenuating flood currents and enhanced ebb currents. However, the effect of river flow on horizontal asymmetry is expected to be much stronger than on $2\phi_{D2}-\phi_{D4}$ (Gallo & Vinzon, 2005). Regarding the effect of tidal range on vertical asymmetry, spring tides undergo higher tidal distortions due to the higher effect of friction (Friedrichs & Aubrey, 1988). In contrast, $2\phi_{D2}-\phi_{D4}$ decreases with higher tidal ranges. This agrees with the fact that $2\phi_{M2}-\phi_{M4}$ falls as the ratio of tidal amplitude to depth increases (Friedrichs & Aubrey, 1988). However, we prefer not to discuss these trends here in depth because the appearance of the fortnightly variability in D_2 and D_4 is related to the use of a wavelet-type tidal analysis approach that does not resolve tidal harmonics but frequency bands, which implies that spring-neap variations appear in higher frequency bands (Hoitink & Jay, 2016; Matte et al., 2014).

5.1.2. Implications of Long-Term Hydrological Changes

As discussed above, river discharge exerts a major effect on the propagation of tides in the GTR, even more significant than in other documented estuaries. This suggests that long-term hydrological changes can impact tidal properties over time, of which the multiannual evolution of tidal properties gives some evidence (Figure 4). However, a comparison of the two hydrologically contrasting years of 2005 (dry) and 2014 (wet) offers an insight into the consequences of decreasing river flow trends, assuming negligible morphological changes (years not too far apart during a period devoid of human morphological changes; Figure 6). At Bordeaux, the dry winter in 2005 (river flow below 930 $m^3\ s^{-1}$, Figure 6a) resulted in an increase in tidal range of up to 0.5 m (9%) and 0.7 m (23%) during spring and neap tides respectively (Figure 6b), compared a wet winter such as in 2014 (flood peaks up to 4,225 $m^3\ s^{-1}$). Concurrently, the maximum tidal distortion A_{D4}/A_{D2} decreased from 0.3 to 0.22 (36%; Figure 6c). Summer 2014 was also wetter than summer 2005; the minimum river flow between June and August 2014, around 215 $m^3\ s^{-1}$, was the maximum value for the same period in 2005 (Figure 6a). A decrease in summer river flow from the values of 2014 to those of 2005 did not seem to impact tidal range at Bordeaux (same maximum value in 2005 and 2014) but decreased tidal distortion by up to 20% during neap tides. Therefore, only major hydrological changes impacted tidal range in the lower GTR, as previously suggested by Figure 5Ic. However, a change in mean summer river flow (for example from 200 ± 50 to $100 \pm 50\ m^3\ s^{-1}$) could induce an important increase in the tidal range at Cadillac (around 11.5%, Figure 5Id). Unlike in the GTR, the interannual decrease in discharge hardly affects the tidal range in the Columbia River due to flow regulation, although future decreases in discharge may drive further changes in the water level (Jay et al., 2011). To our knowledge, there are no other studies addressing the impact of long-term hydrological changes on tides and, as a consequence, we have no comparative values for a further discussion of our results.

5.2. Impact of Morphology on the Evolution of Tides

Having established the effect of river flow, we now focus on the impact of morphological changes on the evolution of tidal properties in the GTR over the last six decades. We recall that the Gironde Estuary underwent moderate morphological changes between its mouth and the confluence of the two tidal rivers unrelated to engineering works and characterized by the upstream shift of the bottom accretion zone between
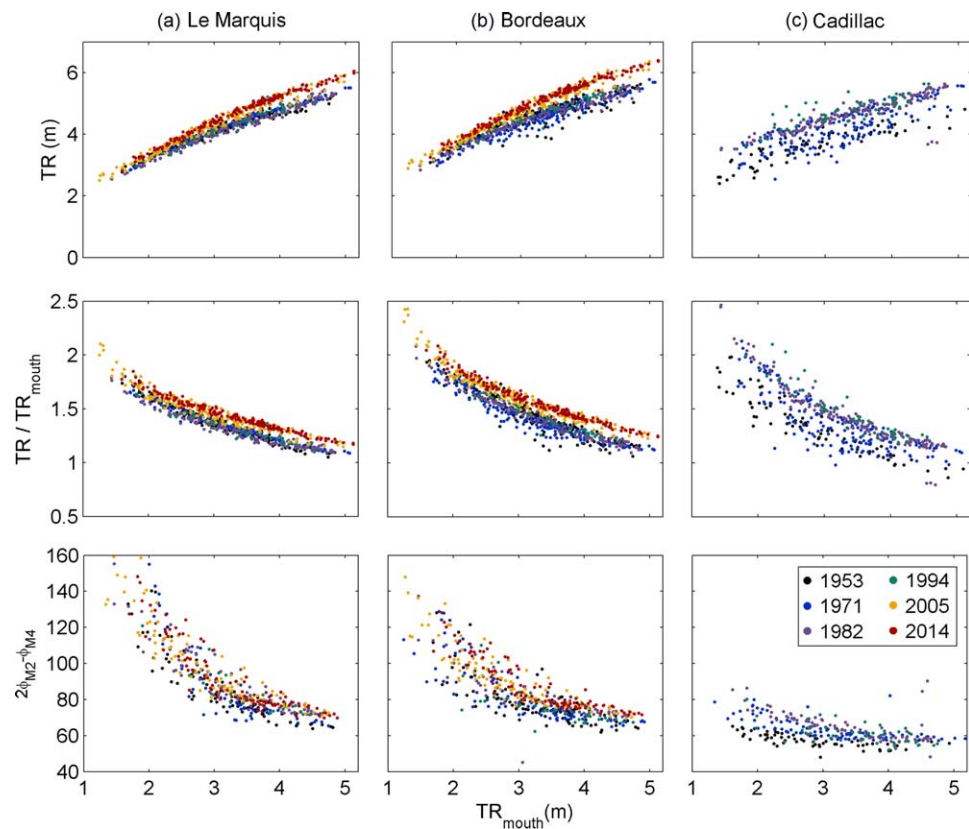
Figure 7. (I) Tidal range (TR), (II) tidal range increase relative to the mouth (TR/TR$_{mouth}$), and (III) tidal asymmetry direction (2ϕ_{D2}-ϕ_{D4}) as a function of tidal range at the mouth (TR$_{mouth}$) for each study year and with a river flow between 100 and 250 m^3 s^{-1} at (a) Le Marquis, (b) Bordeaux, and (c) Cadillac.

1962 and 1994 (Sottolichio et al., 2013). The GTR was instead subject to gravel extractions between 1956 and 1980 from Bordeaux to its upstream limit. These human interventions deepened several sections, suppressed intertidal zones and reduced bottom roughness. In order to filter out the effect of river flow, and thus isolate the influence of morphology, the multidecadal evolution of tidal range, tidal range increase and tidal asymmetry direction are plotted for a narrow range of river flows (100 m^3 s^{-1} < Q < 250 m^3 s^{-1}) in Figures 7I–7III. This range is representative of all the study years (Figure 2), and groups the lowest possible values, thereby filtering out the influence of river flow. Tidal distortion was not included because it remains roughly constant over time (Figure 4III). Table 1 shows the percentage changes in the tidal parameters between each study year and the accumulated percentages of these changes over a period during which TR$_{mouth}$ was 4–4.5 m.

Table 1

Percentage Change of Tidal Range (TR) and Tidal Asymmetry Direction (2ϕ_{D2}-ϕ_{D4}) in the Periods Between Study Years at Le Marquis, Bordeaux, and Cadillac

Parameter	Station	1953–1971	1971–1982	1982–1944	1994–2005	2005–2014
TR	Le Marquis	+3.1% (+3.1%)	−1.6% (+1.5%)	+1% (+2.5%)	**+7.3%** (+9.8%)	+2.1% (±11.9%)
	Bordeaux	+1.4% (+1.4%)	+1% (+2.4%)	+1.4% (+3.8%)	**+9.2%** (+13%)	+1.9% (±14.9%)
	Cadillac	**+17.1%** (+17.1%)	+5.2% (+22.3%)	+0.8% (±23.1%)		
2ϕ_{D2}-ϕ_{D4}	Le Marquis	+3.8% (+3.8%)	**+6.5%** (+10.3%)	−0.7% (9.6%)	+3.4% (13%)	−0.3% (±12.7%)
	Bordeaux	+5% (+5%)	**+5.9%** (+10.9%)	−2.6% (+8.3%)	+4.9% (+13.2%)	+2% (±15.2%)
	Cadillac	**+10.1%** (+10.1%)	−0.3% (+9.8%)	−0.2% (±9.6%)		

Note. Accumulated percentages are given in parentheses. Bold numbers highlight the most important changes at each station. Underlined percentages indicate the total variation between 1953 and 2014 for Le Marquis and Bordeaux (1953 and 1994 for Cadillac). Data correspond to river flows between 100 and 250 m^3 s^{-1} and tidal ranges at the mouth between 4 and 4.5 m.

In general, morphological changes have led to a progressive increase in TR and $2\phi_{D2}$-ϕ_{D4} in the GTR, especially at Cadillac (Figure 7I and Table 1). At Le Marquis and Bordeaux (Figures 7Ia and 7Ib), TR showed a slight but constant increase between 1953 and 1994, on average below 0.2 m (2.5% at Le Marquis and 3.8% at Bordeaux), but up to a maximum of 0.5 m. Then, between 1994 and 2005, TR increased further, around 0.4–0.5 m on average (9.8% at Le Marquis and 13.1% at Bordeaux). In total, the increase in TR attributed to morphologal changes was of 0.6 m on average (12–15%, up to 1.3 m at Bordeaux) in the lower GTR between 1953 and 2014. So for example, a TR_{mouth} of 4–4.5 m was amplified in the estuary by a factor of 1.1–1.2 in 1953 and by a factor of 1.3–1.4 in 2014 (Figures 7IIa and 7IIb). The amplification factor decreased with tidal range at the mouth, as spring tides are more affected by friction and hence relatively less amplified (Bonneton et al., 2015; Wang et al., 2014). The amplification over time of the tidal asymmetry direction at Le Marquis and Bordeaux also followed similar trends at Le Marquis and Bordeaux (Figures 7IIIa and 7IIIb and Table 1). For a tidal range of 4–4.5 m, $2\phi_{D2}$-ϕ_{D4} increased from 66° to 77° on average between 1953 and 2014 (13–15%), with the biggest increase between 1971 and 1982.

At Cadillac, TR experienced a larger increase between 1956 and 1994 than Le Marquis and Bordeaux: 1 m on average (24%) and up to a maximum of 1.4 m (Figure 7Ic). In terms of amplification in the estuary, a tidal wave of 4 m amplitude at the mouth had the same amplitude at Cadillac in 1953, but in 1994 it was multiplied by a factor of 1.3 there (Figure 7IIc). Unlike at Le Marquis and Bordeaux, where TR increased at a roughly constant rate between the 1950s and the 1990, most of the change in TR at Cadillac was concentrated between the 1950s and the 1970s, concurrent with the period of gravel extraction in the upper GTR. Tidal asymmetry direction also reached its greatest increase during this period (from 53.5° to 59°, 10%); it then remained roughly constant until 1994. These different patterns suggest that the moderate and natural morphological changes in the Gironde Estuary were responsible for the increase in tidal range (2.5–4% between 1953 and 1994; 12–15% between 1953 and 2014, Table 1) and tidal asymmetry direction (8–10% between 1953 and 1994; 13–15% between 1953 and 2014, Table 1) in the lower GTR. However, gravel extraction in the upper GTR caused higher rates of increase in the tidal range (23% between 1956 and 1994, Table 1) and asymmetry direction (10% between 1956 and 1994, Table 1) in the region of Cadillac, a consequence of the loss of intertidal zones and the decrease in bottom roughness (Winterwerp & Wang, 2013).

This work has shown that morphological changes in the Gironde Estuary have resulted in significant increases in tidal range and asymmetry direction between 1953 and 2014 in the GTR. These increases were, however, quite moderate compared with estuaries undergoing continuous interventions. For example, the Ems Estuary experienced a tidal range amplification of 125% at the mouth between 1950 (1.6 m) and 2010 (3.6 m), mainly due to continuous channel deepening (van Maren et al., 2015). From semianalytical simulations in this same estuary, Chernetsky et al. (2010) found that flood dominance, in terms of $2\phi_{M2}$-ϕ_{M4}, increased by up to 18% between 1980 and 2005 in the upper reaches, but decreased by 7% in the lower estuary. Similarly, the progressive narrowing of the Loire Estuary increased the tidal range in the lower reaches by 360% between 1904 (1.2 m) and 2004 (5.5 m; Winterwerp et al., 2013). In the Western Scheldt, deepening of the upper region increased the tidal range (by up to 40% between 1901 and 2013) but reduced the flood dominance (Winterwerp et al., 2013). Most of these studies found also that increased tidal range and asymmetry significantly favor the upstream net transport of fine sediments.

5.3. Impact of TMZ-Related Mobile Mud

We have demonstrated that tidal range and asymmetry direction have increased over the last six decades in the GTR due to the combined impact of natural and human-induced morphological changes. The increase in these two parameters was even more pronounced during dry years, and slightly mitigated during wet years; vertical tidal distortion increased, particularly in the upper reaches of the GTR. Despite the lack of morphological data, the upstream displacement of the turbidity maximum zone (TMZ) seems to be the main responsible for the natural morphological changes in the Gironde (Sottolichio et al., 2013); the intensity of the TMZ has increased in the GTR over the last decades, due in particular to the multidecadal decrease in river flow (Jalón-Rojas et al., 2015). However, given that increasing tidal range and asymmetry intensify fine sediment resuspension and transport up-estuary by tidal pumping (de Jonge et al., 2014; Uncles et al., 2002; Winterwerp et al., 2013), the multidecadal evolution of the tides could also be responsible for the intensification of the TMZ in the upper reaches.

Winterwerp and Wang (2013) found that increasing fine sediments can reduce the effective hydraulic drag (decreasing bottom roughness and/or damping turbulence), which then enhances in lockstep tidal range and therefore turbidity. In the case of the Gironde fluvio-estuarine system, mobile mud can form when the TMZ is positioned in the lower reaches of the GTR. The mobile mud may remain on place during a dry winter but is expelled by river floods in wet years (Jalón-Rojas et al., 2015). The presence of the mud then could reduce the effective hydraulic drag so increase tidal range. In order to verify this hypothesis, the amplification factor TR/TR_{mouth} at Le Marquis and Bordeaux is plotted against TR_{mouth} in Figure 8, distinguishing between the periods before and after the presence of the turbidity maximum for a given year. Both periods were characterized by a river flow between 300 and 700 $m^3 s^{-1}$. The comparison is plotted for two dry years (1953 and 2005) and two wet years (1994 and 2014). While the tidal range amplification shows similar values before and after the occurrence of turbidity maximum during dry years, it is lower before the presence of the turbidity maximum in wet years. For example, a tidal wave of 4 m at the mouth is amplified at Bordeaux by factors of 1.25 and 1.5, respectively, after and before the occurrence of the turbidity maximum at this section (factors of 1.3 and 1.4 for 2014). Note that changes in bottom friction are not related to aquatic plants in the GTR because the high levels of turbidity limit light penetration and therefore photosynthetic activity (Irigoien & Castel, 1997).

The values of TR/TR_{mouth} during dry years are of the same order of magnitude as after the ocurrence of the turbidity maximum in wet periods (dotted lines, Figure 8). The river flow during dry winters is not enough to expel the mobile mud remaining from the previous event of turbidity maximum during low water periods, leading to persistent muddy beds that strengthen the tidal range amplification over the whole year. Wet years are instead characterized by the seasonal presence of mobile mud, only after the passage of the turbidity maximum; this reduces bottom roughness and enhance tidal range with respect to periods before such passage. This seasonal variability occurs at Le Marquis and Bordeaux during very wet years like 1994, but only at Bordeaux in 2014, indicating that there is a permanent presence of mobile mud at Le Marquis. This suggests that, during dry years, there may exist a seasonal variation in bottom roughness and tidal wave amplification in sections upstream of Bordeaux. No impact of the seasonal variation in bottom roughness was found on tidal asymmetry direction (figure not shown). Such a seasonal variability of tidal range amplification has only been previously documented in the Guadalquivir River (Wang et al., 2014) but, contrary to the Gironde, there TR/TR_{mouth} raises with the increasing suspended sediment concentration induced by river floods.

5.4. Implications of the Evolution of Tides in an Estuarine System

In summary, the hydrosedimentary behavior of the Gironde fluvio-estuarine system over the last decades has involved several feedback mechanisms that may favor the intensification of tides and of the turbidity maximum up-estuary (Figure 9):
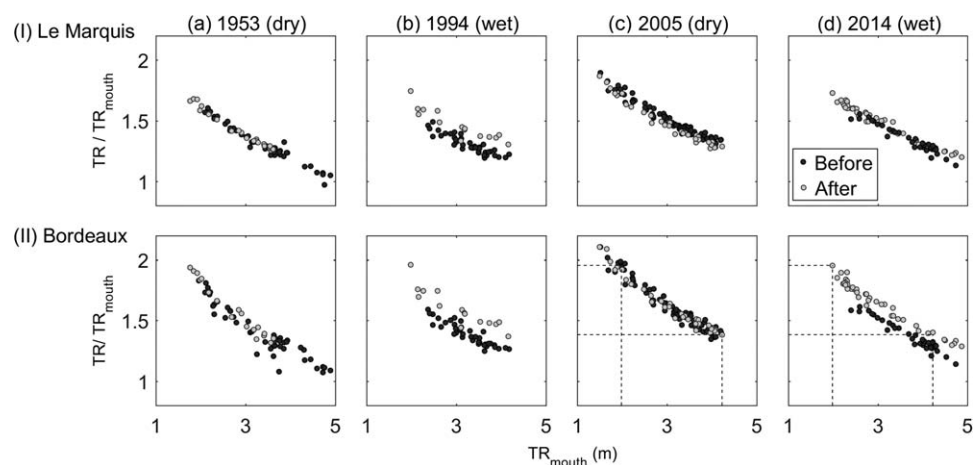

Figure 8. Tidal range amplification (TR/TR_{mouth}) as a function of tidal range at the mouth (TR_{mouth}) at (I) Le Marquis and (II) Bordeaux for periods before (black points) and after (white circles) the TMZ occurrence in 1953, 1994, 2005, and 2014. Data correspond to periods of river flow between 300 and 700 $m^3 s^{-1}$. Dotted lines help compare dry and wet years.
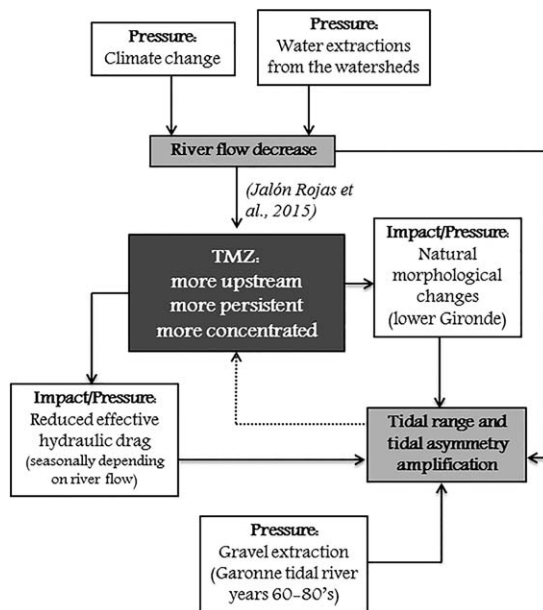
Figure 9. Schematic diagram of the interactions between environmental and human pressures, and their consequences for the hydrosedimentary dynamics of the Garonne Tidal River between the 1950s and the present. The feedback of tidal range and asymmetry to the TMZ (dotted arrow) is a hypothesis, which needs to be tested by further modeling.

1. Climate change and the intensification of water abstraction in the watershed result in decreasing river discharge, enhancing not only the concentration, persistence, and upstream displacement of the turbidity maximum (see details in Jalón-Rojas et al., 2015) but also the tidal range and asymmetry direction.

2. The upstream shifts of the turbidity maximum reduce bottom roughness and generate permanent morphological changes. This also contribute to the increases in tidal range and asymmetry direction.

3. The gravel extraction between the 1960s and the 1980s deepened sections, eliminated intertidal zones, and led to smoother beds. As a consequence, the tidal range and asymmetry direction increased in the region of Cadillac.

4. The increases in tidal range and asymmetry due to these processes have likely contributed to more intense tidal pumping and therefore the intensification of the turbidity maximum; this, in turn, causes changes in morphology and bottom roughness.

The fact that the tidal range and asymmetry changes have significantly impacted sediment advection and the turbidity maximum is at this stage a hypothesis. In this work, we have only evaluated the evolution of vertical asymmetry, but it is the horizontal asymmetry that governs the residual transport of sediments. However, given that the vertical asymmetry direction can be a good indicator of horizontal asymmetry (Neill et al., 2014), we assume that there was an intensification of flood conditions over the last decades that would have contributed to the upstream shift of the turbidity maximum. This assumption needs to be tested by further modeling.

The outcomes of this work are particularly crucial for better forecasting the evolution of tidal propagation in the Gironde fluvio-estuarine system. Given that the annual discharge of the Garonne is projected to decrease, as in other south European river basins (Alfieri et al., 2015), tidal range and asymmetry direction are expected to continue increasing, for three reasons: (a) the direct impact of decreasing river flow on these parameters, particularly in the upper reaches, (b) the upstream shift of the turbidity maximum and therefore of the accretion zone due to decreasing discharges, and (c) the longer presence of seasonal mobile mud in the upper reaches, promoted by persistent low discharges. By analogy, therefore, one could speculate that the predicted decreasing trends in discharge in different world regions are likely to influence tidal propagation in many estuaries, in particular those having a TMZ.

No study has evaluated jointly the effects of river flow and morphology on the evolution of tides so far. Most estuaries for which the interannual evolution of tides was assessed are characterized by major human-induced morphological changes and discharges regulated by weirs (e.g., Ems, Scheldt, Weser Rivers; van Maren et al., 2015; Winterwerp et al., 2013). Even so, the generation of overtides and subtidal dynamics is reliant on river flow in regulated estuaries, as shown by Losada et al. (2017) on the Guadalquivir. Therefore, the evaluation of multidecadal changes in tides should consider both discharge and morphological impacts. Furthermore, the present work highlights methodological implications, such as the relevance of developing and improving the modeling of tidal-river dynamics (e.g., Cai et al., 2014) and nonstationary harmonic methods such as NS_TIDE (Matte et al., 2013). Studies using NS_TIDE or regression methods (Kukulka & Jay, 2013) to forecast tides from future trends in river flows should use only the most up-to-date tide data, and consider as a limitation that even moderate natural morphological changes could impact the evolution of tides. In addition, the modeling of estuaries characterized by a seasonal variation in the turbidity maximum and in the mobile mud should include a time-varying effective hydraulic drag in order to improve the prediction of tides and therefore of suspended sediment concentrations.

6. Conclusions

This study has quantified the changes in tidal range and vertical tidal asymmetry over the last six decades in the Garonne Tidal River (GTR), the upper region of the Gironde Estuary, a consequence of changes in
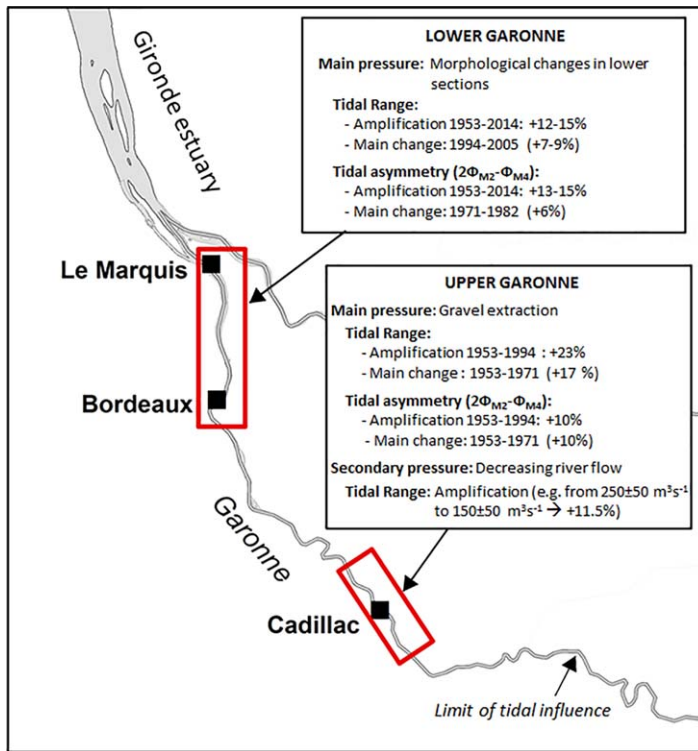
Figure 10. Summary of the main modifications in tidal characteristics in the tidal Garonne River for the period 1953–2014.

hydrology (seasonal and multidecadal changes) and in natural morphology (upstream shift of the accretion zone due to hydrological changes), and of gravel extraction (which deepened sections, removed intertidal zones and decreased bed roughness).

Observations revealed that both the tidal range (TR) and asymmetry direction $2\phi_{D2}-\phi_{D4}$ in the GTR have increased over the last six decades. The increase in $2\phi_{D2}-\phi_{D4}$ suggests an intensification of flood dominant conditions with time. Three factors affect TR evolution: river flow; morphology; and bottom roughness (at both seasonal and interannual time scales); the increase in $2\phi_{D2}-\phi_{D4}$ was mainly the result of interannual changes in morphology and bottom roughness.

Both TR and $2\phi_{D2}-\phi_{D4}$ have increased progressively over the decades in the lower GTR (around Le Marquis and Bordeaux, Figure 10), up to an average increase of 12–15% between 1953 and 2014 for dry periods. The similar rates of change during periods with and without gravel extraction suggest that this increase was mainly promoted by natural morphological changes. River flow also influences TR in the lower GTR. On a seasonal scale, TR can increase by 15% from river floods periods (1,500–2,000 m³ s⁻¹) to dry periods (100–200 m³ s⁻¹). The annual trends in TR depend similarly on the hydrological regime. The hydrological regime also induces seasonal changes of bottom roughness that affect TR. Dry years were characterized by the persistence of mobile mud in the lower GTR (after the departure of the TMZ) that increased TR up to 16% compared to periods of absence of these deposits during the winter and spring of wet years.

The evolution of TR and $2\phi_{D2}-\phi_{D4}$ followed different patterns in the upper GTR (around Cadillac, Figure 10). The increase in these parameters was higher than in the lower sections (Le Marquis and Bordeaux); the most significant change occurred between 1956 and 1971, concurrent with gravel extraction. Between 1956 and 1994, TR and $2\phi_{D2}-\phi_{D4}$ increased on average by 17% and 10%, respectively, of which around 3–4% would have been consequence of natural morphological changes in the Gironde (values in the lower section of the GTR). Therefore, the changes in morphology and bottom roughness induced by gravel extraction were the main factors that affected tidal properties in the last decades. Hydrology also plays a major role in the evolution of tides in the upper GTR. A slight decrease in river flow can increase tidal range significantly (e.g., +11.5% from 200–300 to 100–200 m³ s⁻¹; Figure 10). Furthermore, decreasing discharges shift the boundary between the river-dominated and tide-dominated regions upriver.

This study is the first to encompass the effects of morphology and hydrology on long-term changes in tides, and the results demonstrate the importance of considering both factors. In the Gironde fluvial-estuarine system, long-term hydrological and morphological changes are intrinsically related, and their feedback contribute to the increases in TR and $2\phi_{D2}-\phi_{D4}$. Decreasing river flow is the main factor explaining the trends of natural morphological changes and of the higher persistence of low bottom roughness in the lower section of the GTR. This implies that tidal range and asymmetry are likely to further increase with the expected decrease in river flow over the next decades.

Future work on estuarine dynamics needs to consider the impact of morphology on tides. This could be achieved by quantifying the morphological changes over time in terms of loss/gain of intertidal zones, accretion/erosion rates, depth variations, and seasonal bottom roughness shifts. Such an analysis is not possible in the GTR due to the scarcity of historical bathymetric and sedimentological data. Another important issue is the implications of the described tidal patterns on the transport of suspended sediments. Besides the decreasing trend in river flow, the amplification of tidal range and vertical asymmetry could have also contributed to the intensification of the turbidity maximum in the GTR, which in turn favors the changes in morphology and bottom roughness that enhance tidal properties.

Table A1
Summary of Advantages and Disadvantages of the Main Tidal Analysis Methods

Type	Method		Advantage	Disadvantage
Stationary	HA		Resolution of tidal constituent (M_2, S_2, M_4, MSf, etc.) Suitable for predictions	No reproduction of time-varying properties such as those characteristic of tidal-river dynamics
Nonstationary	Short-term HA		Resolution of tidal constituent (M_2, S_2, M_4, MSf, etc.)	Inaccurate results when river flow variability is high (Jay & Flinchem, 1997) Not suitable for prediction
	NS-HA		Resolution of tidal constituent (M_2, S_2, M_4, MSf, etc.) Suitable for predictions Accurate in determining time variations of tidal constituents	Need for long records (Matte et al., 2013) The model reaches its limits for very low river flows? Relies on the availability of river flow records
	Wavelet approach	Complex demodulation (single frequency) CWT (multifrequency)	Accurate in coping with nontidal variations and strong time-varying properties (Guo et al., 2015)	No resolution of tidal constituent, but frequency bands (diurnal, semidiurnal, etc.). This implies that spring-neap variations appear in higher frequency bands (Hoitink & Jay, 2016) Not suitable for prediction, unless it is used in a prediction model (Kukulka & Jay, 2003)

Appendix A: Brief Overview of Tidal Analysis Methods

There are two groups of methods for determining amplitudes and phases of the frequencies involved in a tidal signal; most of them are described in the methods state of art provided by Hoitink and Jay (2016): (a) stationary methods, such as classical harmonic analysis (Pawlowicz et al., 2002), which are suitable for oceanic tides in deep waters and (b) nonstationary methods, which are better suited to tidal rivers subject to nonstationary forcing such as river flow. Nonstationary methods include short-time harmonic analysis (Godin, 1999; Guo et al., 2015; Zaron & Jay, 2014), nonstationary harmonic analysis (Matte et al., 2013), and wavelet approaches (complex demodulation, Gasquet & Wootton, 1997; continuous wavelet transform, Jay & Flinchem, 1997, 1999).

The main advantages and disadvantages of these methods are briefly summarized in Table A1.

References

Alebregtse, N. C., & de Swart, H. E. (2016). Effect of river discharge and geometry on tides and net water transport in an estuarine network, an idealized model applied to the Yangtze Estuary. *Continental Shelf Research*, *123*, 29–49. https://doi.org/10.1016/j.csr.2016.03.028

Alfieri, L., Burek, P., Feyen, L., & Forzieri, G. (2015). Global warming increases the frequency of river floods in Europe. *Hydrology and Earth System Sciences*, *19*(5), 2247–2260. https://doi.org/10.5194/hess-19-2247-2015

Allen, G. P., Salomon, J. C., Bassoullet, P., Du Penhoat, Y., & De Grandpré, C. (1980). Effects of tides on mixing and suspended sediment transport in macrotidal estuaries. *Sedimentary Geology*, *26*, 69–90.

Barendregt, A., & Swarth, C. W. (2013). Tidal freshwater wetlands: Variation and changes. *Estuaries and Coasts*, *36*(3), 445–456. https://doi.org/10.1007/s12237-013-9626-z

Bloomfield, P. (2004). *Fourier analysis of time series: An introduction. Wiley series in probability and statistics*. Hoboken, NJ: John Wiley. https://doi.org/10.2307/2344882

Boé, J., Terray, L., Martin, E., & Habets, F. (2009). Projected changes in components of the hydrological cycle in French river basins during the 21st century. *Water Resources Research*, *45*, W08426. https://doi.org/10.1029/2008WR007437

Bonneton, P., Bonneton, N., Parisot, J.-P., & Castelle, B. (2015). Tidal bore dynamics in funnel-shaped estuaries. *Journal of Geophysical Research: Oceans*, *120*, 923–941. https://doi.org/10.1002/2014JC010267

Boon, J. D. (1992). Temporal variation of shallow-water tides in basin-inlet systems. In *Hydrodynamics and sediment dynamics of tidal inlets*. (pp. 125–136). https://doi.org/10.1029/LN029p0125

Caballero, Y., Voirin-Morel, S., Habets, F., Noilhan, J., LeMoigne, P., Lehenaff, A., et al. (2007). Hydrological sensitivity of the Adour-Garonne river basin to climate change. *Water Resources Research*, *43*, W07448. https://doi.org/10.1029/2005WR004192

Cai, H., Savenije, H. H. G., & Toffolon, M. (2012). A new analytical framework for assessing the effect of sea-level rise and dredging on tidal damping in estuaries. *Journal of Geophysical Research*, *117*, C09023. https://doi.org/10.1029/2012JC008000

Cai, H., Savenije, H. H. G., & Toffolon, M. (2014). Linking the river to the estuary: Influence of river discharge on tidal damping. *Hydrology and Earth System Sciences*, *18*(1), 287–304. https://doi.org/10.5194/hess-18-287-2014

Castaing, P., & Allen, G. P. (1981). Mechanisms controlling seaward escape of suspended sediment from the Gironde: A macrotidal estuary in France. *Marine Geology*, *40*, 101–118.

Castaing, P., Etcheber, H., Sottolichio, A., & Cappe, R. (2006). *Evaluation de l'évolution hydrologique et sédimentaire du système Garonne-Dordogne-Gironde*. Bordeaux, France: Agence de l'eau Adour-Garonne, Université de Bordeaux.

Chernetsky, A. S., Schuttelaars, H. M., & Talke, S. A. (2010). The effect of tidal asymmetry and temporal settling lag on sediment trapping in tidal estuaries. *Ocean Dynamics*, *60*(5), 1219–1241. https://doi.org/10.1007/s10236-010-0329-8

Chevalier, L., Laignel, B., Massei, N., Munier, S., Becker, M., Turki, I., et al. (2014). Hydrological variability of major French rivers over recent decades, assessed from gauging station and GRACE observations. *Hydrological Sciences Journal*, *59*(10), 1844–1855. https://doi.org/10.1080/02626667.2013.866708

de Jonge, V. N., Schuttelaars, H. M., van Beusekom, J. E. E., Talke, S. A., & De-Swart, H. E. (2014). The influence of channel deepening on estuarine turbidity levels and dynamics, as exemplified by the Ems estuary. *Estuarine, Coastal and Shelf Science*, *139*, 46–59. https://doi.org/10.1016/j.ecss.2013.12.030

Dronkers, J. (1992). Tide-induced residual transport of fine sediment. In *Physics of shallow estuaries and bays* (pp. 228–244). New York, NY: Springer. https://doi.org/10.1029/LN016p0228

ESRI. (2014). *ArcGIS desktop: Release 10.3*. Redlands, CA: Author.

Fortunato, A. B., & Oliveira, A. (2005). Influence of intertidal flats on tidal asymmetry. *Journal of Coastal Research*, *215*, 1062–1067. https://doi.org/10.2112/03-0089.1

Friedrichs, C. T. (2010). Barotropic tides in channelized estuaries. In A. Valle-Levinson (Ed.), *Contemporary issues in estuarine physics*. Cambridge, UK: Cambridge University Press.

Friedrichs, C. T., & Aubrey, D. G. (1988). Non-linear tidal distortion in shallow well-mixed estuaries: A synthesis. *Estuarine, Coastal and Shelf Science*, *27*(5), 521–545. https://doi.org/10.1016/0272-7714(88)90082-0

Friedrichs, C. T., & Aubrey, D. G. (1994). Tidal propagation in strongly convergent channels. *Journal of Geophysical Research*, *99*(C2), 3321–3336. https://doi.org/10.1029/93JC03219

Gallo, M. N., & Vinzon, S. B. (2005). Generation of overtides and compound tides in Amazon estuary. *Ocean Dynamics*, *55*, 441–448. https://doi.org/10.1007/s10236-005-0003-8

Gasquet, H., & Wootton, A. J. (1997). Variable-frequency complex demodulation technique for extracting amplitude and phase information. *Review of Scientific Instruments*, *68*(1), 1111–1114.

Godin, G. (1985). Modification of river tides by the discharge. *Journal of Waterway, Port, Coastal, and Ocean Engineering*, *111*(2), 257–274. https://doi.org/10.1061/(ASCE)0733-950X(1985)111:2(257)

Godin, G. (1991). Frictional effects in river tides. In B. B. Parker (Ed.), *Tidal hydrodynamics* (pp. 379–402). Toronto, Canada: John Wiley.

Godin, G. (1999). The propagation of tides up rivers with special considerations on the Upper Saint Lawrence River. *Estuarine, Coastal and Shelf Science*, *48*(3), 307–324. https://doi.org/10.1006/ecss.1998.0422

Guo, L., Van-der-Wegen, M., Jay, D. A., Matte, P., Wang, Z. B., Roelvink, D., et al. (2015). River-tide dynamics: Exploration of nonstationary and nonlinear tidal behavior in the Yangtze River estuary. *Journal of Geophysical Research: Oceans*, *120*, 3499–3521. https://doi.org/10.1002/2014JC010491

Guo, L., Van-der-Wegen, M., Roelvink, J. A., & He, Q. (2014). The role of river flow and tidal asymmetry on 1-D estuarine morphodynamics. *Journal of Geophysical Research: Earth Surface*, *119*, 2315–2334. https://doi.org/10.1002/2014JF003110

Guo, L., Van-der-Wegen, M., Wang, Z. B., & He, Q. (2016). Exploring the impacts of multiple tidal constituents and varying river flow on long-term, large-scale estuarine morphodynamics by means of a 1-D model: Estuarine morphodynamics. *Journal of Geophysical Research: Earth Surface*, *121*, 1000–1022. https://doi.org/10.1002/2016JF003821

Henrie, K., & Valle-Levinson, A. (2014). Subtidal variability in water levels inside a subtropical estuary. *Journal of Geophysical Research: Oceans*, *119*, 7483–7492. https://doi.org/10.1002/2014JC009829

Hoitink, A. J. F., & Jay, D. A. (2016). Tidal river dynamics: Implications for deltas. *Reviews of Geophysics*, *54*, 240–272. https://doi.org/10.1002/2015RG000507

Horrevoets, A. C., Savenije, H. H. G., Schuurman, J. N., & Graas, S. (2004). The influence of river discharge on tidal damping in alluvial estuaries. *Journal of Hydrology*, *294*(4), 213–228. https://doi.org/10.1016/j.jhydrol.2004.02.012

Huybrechts, N., & Villaret, C. (2013). Large-scale morphodynamic modeling of the Gironde estuary, France. *Proceedings of the ICE - Maritime Engineering*, *166*, 51–62.

Irigoien, X., & Castel, J. (1997). Light limitation and distribution of chlorophyll pigments in a highly turbid estuary: The Gironde (SW France). *Estuarine, Coastal and Shelf Science*, *44*(4), 507–517. https://doi.org/10.1006/ecss.1996.0132

Jalón-Rojas, I., Schmidt, S., & Sottolichio, A. (2015). Turbidity in the fluvial Gironde Estuary (southwest France) based on 10-year continuous monitoring: Sensitivity to hydrological conditions. *Hydrology and Earth System Sciences*, *19*, 2805–2819. https://doi.org/10.5194/hess-19-2805-2015

Jalón-Rojas, I., Schmidt, S., & Sottolichio, A. (2017). Comparison of environmental forcings affecting suspended sediments variability in two macrotidal, highly-turbid estuaries. *Estuarine, Coastal and Shelf Science*, *198*(B), 529–541. https://doi.org/10.1016/j.ecss.2017.02.017

Jay, D. A., & Flinchem, E. P. (1997). Interaction of fluctuating river flow with a barotropic tide: A demonstration of wavelet tidal analysis methods. *Journal of Geophysical Research*, *102*(C3), 5705–5720. https://doi.org/10.1029/96JC00496

Jay, D. A., Leffler, K., & Degens, S. (2011). Long-term evolution of Columbia River Tides. *Journal of Waterway, Port, Coastal, and Ocean Engineering*, *137*(4), 182–191.

Kukulka, T., & Jay, D. A. (2003). Impacts of Columbia River discharge on salmonid habitat: 1. A nonstationary fluvial tide model. *Journal of Geophysical Research*, *108*(C9), 3293. https://doi.org/10.1029/2002JC001382

Lanzoni, S., & Seminara, G. (1998). On tide propagation in convergent estuaries. *Journal of Geophysical Research*, *103*(C13), 30793–30812. https://doi.org/10.1029/1998JC900015

Lanzoni, S., & Seminara, G. (2002). Long-term evolution and morphodynamic equilibrium of tidal channels. *Journal of Geophysical Research*, *107*(C1), 3001. https://doi.org/10.1029/2000JC000468

LeBlond, P. H. (1991). Tides and their interactions with other oceanographic phenomena in shallow water (review). In B. B. Parker (Ed.), *Tidal hydrodynamics* (pp. 357–378). New York, NY: John Wiley.

Losada, M. Á., Díez-Minguito, M., & Reyes-Merlo, M. Á. (2017). Tidal-fluvial interaction in the Guadalquivir River Estuary: Spatial and frequency-dependent response of currents and water levels. *Journal of Geophysical Research: Oceans*, *122*, 847–865. https://doi.org/10.1002/2016JC011984

Matte, P., Jay, D. A., & Zaron, E. D. (2013). Adaptation of classical tidal harmonic analysis to nonstationary tides, with application to river tides. *Journal of Atmospheric and Oceanic Technology*, *30*(3), 569–589. https://doi.org/10.1175/JTECH-D-12-00016.1

Matte, P., Secretan, Y., & Morin, J. (2014). Temporal and spatial variability of tidal-fluvial dynamics in the St. Lawrence fluvial estuary: An application of nonstationary tidal harmonic analysis. *Journal of Geophysical Research: Oceans*, *119*, 5724–5744. https://doi.org/10.1002/2014JC009791

Matte, P., Secretan, Y., & Morin, J. (2017). Hydrodynamic modeling of the St. Lawrence Fluvial Estuary. II: Reproduction of spatial and temporal patterns. *Journal of Waterway, Port, Coastal, and Ocean Engineering*, *143*(5), 1–13. https://doi.org/10.1061/(ASCE)WW.1943-5460.0000394

Mazzega, P., Therond, O., Debril, T., March, H., Sibertin-Blanc, C., Lardy, R., et al. (2014). Critical multi-level governance issues of integrated modelling: An example of low-water management in the Adour-Garonne basin (France). *Journal of Hydrology*, *519*, 2515–2526. https://doi.org/10.1016/j.jhydrol.2014.09.043

Moore, R. D., Wolf, J., Souza, A. J., & Flint, S. S. (2009). Morphological evolution of the Dee Estuary, Eastern Irish Sea, UK: A tidal asymmetry approach. *Geomorphology*, *103*(4), 588–596. https://doi.org/10.1016/j.geomorph.2008.08.003

Neill, S. P., Hashemi, M. R., & Lewis, M. J. (2014). The role of tidal asymmetry in characterizing the tidal energy resource of Orkney. *Renewable Energy*, *68*, 337–350. https://doi.org/10.1016/j.renene.2014.01.052

Nidzieko, N. J. (2010). Tidal asymmetry in estuaries with mixed semidiurnal/diurnal tides. *Journal of Geophysical Research*, *115*, C08006. https://doi.org/10.1029/2009JC005864

Nidzieko, N. J., & Ralston, D. K. (2012). Tidal asymmetry and velocity skew over tidal flats and shallow channels within a macrotidal river delta. *Journal of Geophysical Research*, *117*, C03001. https://doi.org/10.1029/2011JC007384

Pawlowicz, R., Beardsley, B., & Lentz, S. (2002). Classical tidal harmonic analysis including error estimates in MATLAB using T_TIDE. *Computers & Geosciences*, *28*(8), 929–937.

Prandle, D. (1985). Classification of tidal response in estuaries from channel geometry. *Geophysical Journal of the Royal Astronomical Society*, *80*(1), 209–221. https://doi.org/10.1111/j.1365-246X.1985.tb05086.x

Ross, L., & Sottolichio, A. (2016). Subtidal variability of sea level in a macrotidal and convergent estuary. *Continental Shelf Research*, *131*, 28–41. https://doi.org/10.1016/j.csr.2016.11.005

Sassi, M. G., & Hoitink, A. J. F. (2013). River flow controls on tides and tide-mean water level profiles in a tidal freshwater river. *Journal of Geophysical Research: Oceans*, *118*, 4139–4151. https://doi.org/10.1002/jgrc.20297

Sassi, M. G., Hoitink, A. J. F., De Brye, B., & Deleersnijder, E. (2012). Downstream hydraulic geometry of a tidally influenced river delta. *Journal of Geophysical Research*, *117*, F04022. https://doi.org/10.1029/2012JF002448

Savenije, H. H. G., Toffolon, M., Haas, J., & Veling, E. J. M. (2008). Analytical description of tidal dynamics in convergent estuaries. *Journal of Geophysical Research*, *113*, C10025. https://doi.org/10.1029/2007JC004408

Schmidt, S., Bernard, C., Escalier, J.-M., Etcheber, H., & Lamouroux, M. (2017). Assessing and managing the risks of hypoxia in transitional waters: A case study in the tidal Garonne River (South-West France). *Environmental Science and Pollution Research*, *24*, 3251–3259.

Schuttelaars, H. M., de Jonge, V. N., & Chernetsky, A. (2013). Improving the predictive power when modelling physical effects of human interventions in estuarine systems. *Ocean & Coastal Management*, *79*, 70–82. https://doi.org/10.1016/j.ocecoaman.2012.05.009

Sottolichio, A., Hanquiez, V., Périnotto, H., Sabouraud, L., & Weber, O. (2013). Evaluation of the recent morphological evolution of the Gironde estuary through the use of some preliminary synthetic indicators. *Journal of Coastal Research*, *65*, 1224–1229. https://doi.org/10.2112/SI65-207.1

Speer, P. E., & Aubrey, D. G. (1985). A study of non-linear tidal propagation in shallow inlet/estuarine systems Part II: Theory. *Estuarine, Coastal and Shelf Science*, *21*(2), 207–224. https://doi.org/10.1016/0272-7714(85)90097-6

Toublanc, F., Brenon, I., Coulombier, T., & Le Moine, O. (2015). Fortnightly tidal asymmetry inversions and perspectives on sediment dynamics in a macrotidal estuary (Charente, France). *Continental Shelf Research*, *94*, 42–54. https://doi.org/10.1016/j.csr.2014.12.009

Uncles, R. J., Stephens, J. A., & Smith, R. E. (2002). The dependence of estuarine turbidity on tidal intrusion length, tidal range and residence time. *Continental Shelf Research*, *22*, 1835–1856. https://doi.org/10.1016/S0278-4343(02)00041-9

van Maren, D. S., Winterwerp, J. C., & Vroom, J. (2015). Fine sediment transport into the hyper-turbid lower Ems River: The role of channel deepening and sediment-induced drag reduction. *Ocean Dynamics*, *65*(4), 589–605. https://doi.org/10.1007/s10236-015-0821-2

Wang, Z. B., Winterwerp, J. C., & He, Q. (2014). Interaction between suspended sediment and tidal amplification in the Guadalquivir Estuary. *Ocean Dynamics*, *64*(10), 1487–1498. https://doi.org/10.1007/s10236-014-0758-x

Winterwerp, J. C., & Wang, Z. B. (2013). Man-induced regime shifts in small estuaries—I: Theory. *Ocean Dynamics*, *63*(11–12), 1279–1292. https://doi.org/10.1007/s10236-013-0662-9

Winterwerp, J. C., Wang, Z. B., van Braeckel, A., van Holland, G., & Kösters, F. (2013). Man-induced regime shifts in small estuaries—II: A comparison of rivers. *Ocean Dynamics*, *63*(11–12), 1293–1306. https://doi.org/10.1007/s10236-013-0663-8

Yoon, B., & Woo, S.-B. (2013). Tidal asymmetry and flood/ebb dominance around the Yeomha channel in the Han River Estuary, South Korea. *Journal of Coastal Research*, *165*(65), 1242–1246. https://doi.org/10.2112/SI65-210.1

Zaron, E. D., & Jay, D. A. (2014). An analysis of secular change in tides at open-ocean sites in the Pacific. *Journal of Physical Oceanography*, *44*(7), 1704–1726.